Available online at www.sciencedirect.com
SCIENCE DIRECT®
Finite Elements in Analysis and Design 40 (2004) 541–554
FINITE ELEMENTS IN ANALYSIS AND DESIGN
www.elsevier.com/locate/finel

The construction of wavelet finite element and its application

Xuefeng Chen*, Shengjun Yang, Junxing Ma, Zhengjia He

School of Mechanical Engineering, Xi'an Jiaotong University, Xi'an 710049, China

Received 17 October 2002; accepted 6 February 2003

Abstract

The two-dimensional wavelet finite element (WFE) is constructed, in which the scaling functions of Daubechies wavelets are adopted as trial functions. In order to overcome the integral difficulty caused by lack of the explicit Daubechies scaling function expression, a new and efficient integral method for stiffness and load matrices is presented. Then the bending characters of a thin plate are studied based on WFE. Numerical tests indicate that the WFE is highly accurate and effective. For engineering application, the internal temperature distribution of office paper used in office machines such as printers and copiers is analyzed by WFE. The results show that WFE has desirable calculation precision while dealing with singularity problems.

Keywords: Daubechies wavelets; Wavelet finite element; Bending plate; Temperature field; Office paper

1. Introduction

It is a key problem to choose the approximate spaces for finite element method (FEM) [1]. The narrow FEM uses the low-order polynomial as approximate space, while the generalized FEM can adopt many other trial functions. Usually, the development of FEM is deeply related to the extension of approximate spaces. Wavelet finite element (WFE) is a vivid example of this development. The dilation and translation of wavelet functions can build any functions of $L^2(\mathbf{R})$, which denotes the vector space of measurable, square-integrable one-dimensional functions $f(x)$, so it has drawn a great deal of attention from scientists and engineers how to apply the wavelet bases to numerical calculation [2,3]. Because of the compactly supported wavelet functions the stiffness matrix is sparse when it is used as trial functions. Moreover, Jaffard and Laurencot [4] have proved that the condition number of WFE is independent of mesh size, which contrasts to traditional h- or p-based FEMs which generate matrix representations whose condition numbers grow like $O(N^p)$ where N is the

* Corresponding author. Tel.: +86-29-266-3689.
E-mail address: chenxf@mail.xjtu.edu.cn (X. Chen).

0168-874X/$ - see front matter
doi:10.1016/S0168-874X(03)00077-5

number of unknowns and p is the polynomial order of the element [5]. So the WFE can avoid numerical instability and slow convergence for iterative solution algorithms. Furthermore, because of the multi-resolution properties of wavelets, some problems can be analyzed by coarse mesh first, and then the better approximation would be obtained adaptively by multi-resolution refining the certain regions. This will provide accurate data with fewer degrees of freedom and computational cost.

However, for Daubechies wavelets lacking the explicit function expression, traditional numerical integrals such as Gauss integrals cannot provide desirable precision. It is a key problem how to calculate the integrals of wavelet functions when they are used as trial functions. The algorithms developed by Dahmen [6] are essentially based on unbounded domains, the general wavelet bases have to be periodized, and the applications of this methods are limited to cases where the problem domain is unbounded or the boundary condition is periodic [18]. To solve finite domain problems, several procedures are proposed. Chen [7] presented a method to calculate integrals on a bounded interval, which is not convenient to form stiffness matrices. Monasse and Perrier [8] derived integral formulae of load vectors through constructing new wavelet bases on the interval. Ko [5] provided another method to calculate one kind of stiffness matrix, but not including load vector. This paper derived an efficient and new method to calculate load vectors on the interval [0,1] with lesser CPU time than algorithms [7], and then gave the formulae to calculate all kinds of stiffness matrices that are necessarily for constructing higher-dimensional WFE.

Ma Junxing [9] has constructed one-dimensional Daubechies wavelet beam element. Yang Shengjun [10] has presented one-dimensional B-spline wavelet element. This paper aims at extending such elements to higher dimensions, and constructs two-dimensional Daubechies wavelet element. Then the bending equations for the thin plate based on WFE are derived, and the corresponding numerical examples are studied.

As we know, the Fourier transform is global and provides a description of the overall regularity of signals, but it is not well adapted for finding the location and the spatial distribution of singularities. This is a major motivation for studying the wavelet transform in mathematics and in applied domains [11]. Compactly supported wavelets are localized in space, which means that the solution can be refined in regions of high gradient, such as local stress concentrations, variable boundary conditions, without having to regenerate the whole mesh. To verify this, the internal temperature distribution of office paper used in office machines such as printers and copiers with suddenly changing boundary condition is studied. The analyses and results of this problem display that the WFE has desirable calculation precision and good local improvement while dealing with singularity problem of large gradient.

2. Daubechies wavelets

Wavelets have emerged in the last decades as a synthesis of ideas from fields as different as electrical engineering, physics and mathematics. Daubechies wavelets [12,13] have beautiful and deep mathematical properties.

The simplest type of wavelet basis is given by dilates and translates of a single one dimensional function $\psi(x)$:

$$\psi_{j,k} := 2^{j/2}\psi(2^j x - k), \quad j,k \in \mathbb{Z}, \tag{1}$$

the wavelet. All wavelet bases are associated with a multi-resolution analysis: this is a framework in which functions f can be considered as a limit of successive approximations

$$f = \lim_{f\to\infty} \mathrm{Proj}_j f, \quad j \in \mathbb{Z}, \tag{2}$$

where the different $\mathrm{Proj}_j f$ correspond to smoothed versions of f with a "smoothing out action radius" of the order of 2^j. There exists a partner function ϕ of the wavelet, the scaling function, used to build spaces V_j:

$$V_j = \mathrm{Span}\{\phi_{j,k}, k \in \mathbb{Z}\}, \tag{3}$$

corresponding to different resolutions (V_j has resolution 2^{-j}). The V_j's are called approximation spaces and the different V_j's are nested in each other

$$\cdots \subset V_j \subset V_{j+1} \subset \cdots , \tag{4}$$

and in each V_j, the $\{\phi_{j,k}\}$ are an orthonormal basis. There may be several choices of ϕ corresponding to a system of approximation spaces. Different choices for ϕ may yield different multi-resolution analyses. Probably the most useful class of scaling functions are those that have compact or finite support. A function has compact support if it is identically zero outside a finite interval. The scaling functions associated with Daubechies's wavelets are not only compactly supported, but also continuous. The supports of the scaling function is

$$\mathrm{Supp}\,\phi_N = [0, 2N-1], \quad N \in Z^+. \tag{5}$$

The size of the support increases linearly with the regularity. Moreover, the wavelet function ψ has N consecutive moments equal to zero, that is the vanishing moment is N:

$$\int_{-\infty}^{+\infty} x^k \psi_N(x)\,\mathrm{d}x = 0, \quad k = 0, \ldots, N-1. \tag{6}$$

Daubechies wavelets are classified according to the number of vanishing moments they have, for example, Daubechies six-order wavelet (D6) denotes that the wavelet function has six vanishing moments. The smoothness of the scaling function and wavelet increases with the number of vanishing moments.

The link with the wavelet basis is given by the following equation:

$$\mathrm{Proj}_{V_{j+1}} f = \sum_k \langle f, \phi_{j+1,k}\rangle \phi_{j+1,k} = \mathrm{Proj}_{V_j} f + \sum_k \langle f, \psi_{j,k}\rangle \psi_{j,k}. \tag{7}$$

Such a coarse-to-fine strategy is useful to refine the finite elements solution. The different nesting and orthonormality properties listed above cause the functions ϕ to be linked via two-scale relation

$$\phi(x) = \sum_{i=0}^{2N-1} p_i \phi(2x - i). \tag{8}$$

Once the filter coefficients p_i have been identified and ϕ has been constructed, then the associated wavelet is given by the formula

$$\psi(x) = \sum_{i=2-2N}^{1} (-1)^i p_{1-i} \phi(2x - i). \tag{9}$$

3. The construction of WFE

Considering a typical variational boundary value problem,

$$a(u,v)=f(v),\quad u\in V,\quad \forall v\in V, \tag{10}$$

where a $(\cdot,\cdot)$ is a coercive, symmetric bilinear form over the Hilbert space.

Supposing that one-dimensional scaling functions $\phi^1(x)$, $\phi^2(x)$ generate multi-resolution analyses $\{V_j^1\}$, $\{V_j^2\}$ respectively, the tensor product space of V_j^1 and V_j^1 is

$$V_j=V_j^1\otimes V_j^2, \tag{11}$$

where $\otimes$ is the Kronecker symbol. The span of V_j^1 is $\{2^{j/2}\phi^1(2^jx-k)\}$ and that of V_j^2 is $\{2^{j/2}\phi^2(2^jx-k)\}$. If we write two-dimensional functions in the form

$$\begin{aligned} &f_{j:k,l}(x,y)=2^jf(2^jx-k,2^jy-l),\\ &\phi(x,y)=\phi^1(x)\phi^2(y), \end{aligned} \tag{12}$$

then $\{\phi_{j:k,l}(x,y)\}$ is the span of V_j. Therefore, $\{V_j\}$ generates a multi-resolution analysis of $L^2(\mathbf{R}^2)$, and $\phi(x,y)$ are scaling functions correspondingly. So the u, v in Eq. (10) can be given by

$$\begin{aligned} &u=\sum_k\sum_l d_{kl}\phi(2^jx-k)\phi(2^jy-l)=\sum_k\sum_l d_{kl}\phi_k\phi_l=\mathbf{\Phi_k}\otimes\mathbf{\Phi_l}\mathbf{d_l},\\ &v=\mathbf{\Phi_k}\otimes\mathbf{\Phi_l}\mathbf{d}_2, \end{aligned} \tag{13}$$

where $\mathbf{d}_1$ and $\mathbf{d}_2$ are the coefficients of wavelet space.

Substituting Eq. (13) into Eq. (10), we would obtain the integrals of scaling functions as follows, which are called connection coefficients:

$$M_k^m=\int_{-\infty}^{+\infty}\chi_{[0,1]}(\xi)\xi^m\phi(\xi-k)\,\mathrm{d}\xi, \tag{14}$$

$$\tau_{k,l}^{m,n}=\int_{-\infty}^{+\infty}\chi_{[0,1]}(\xi)\phi^{(m)}(\xi-k)\phi^{(n)}(\xi-l)\,\mathrm{d}\xi. \tag{15}$$

These coefficients will form load vectors and stiffness matrices of WFE. The details are discussed in the following section. In order to calculate these integrals, we use the definition of characteristic function [5]

$$\chi_{[0,1]}(\xi)=\begin{cases}1, & 0\leqslant\xi\leqslant1,\\ 0 & \text{otherwise}\end{cases} \tag{16}$$

which satisfies a simple two-scale relation

$$\begin{aligned} \chi_{[0,1]}\left(\tfrac{1}{2}\zeta\right)&=\chi_{[0,1]}(\zeta)+\chi_{[1,2]}(\zeta)\\ &=\chi_{[0,1]}(\zeta)+\chi_{[0,1]}(\zeta-1). \end{aligned} \tag{17}$$

Substituting Eq. (8) into Eq. (14), we obtain

$$M_k^m = \sum_i p_i \int_{-\infty}^{+\infty} \chi_{[0,1]}(\xi)\xi^m \phi(2\xi - 2k - i)\,\mathrm{d}\xi$$

$$= \frac{1}{2^{m+1}} \sum_i p_i \int_{-\infty}^{+\infty} \gamma^m [\chi_{[0,1]}(\gamma) + \chi_{[0,1]}(\gamma - 1)]\phi(\gamma - 2k - i)\,\mathrm{d}\gamma$$

$$= \frac{1}{2^{m+1}} \sum_i p_i \left(M_{2k+i}^m + \sum_{s=0}^{m} \binom{m}{s} M_{2k+i-1}^{m-s} \right). \tag{18}$$

We calculate the moments M_k^m by induction on m, so we assume that M_k^s has already been calculated for all k, for all $s < k$. For $s = 0$, we have

$$M_k^0 = \frac{1}{2} \sum_i p_i (M_{2k+i}^0 + M_{2k+i-1}^0)$$

$$= \frac{1}{2} \sum_r (p_{r-2k} + p_{r-2k+1}) M_r^0, \tag{19}$$

expressing in matrix form

$$\left(\frac{1}{2}\mathbf{P} - \mathbf{I} \right) \mathbf{M}^0 = \mathbf{0}, \tag{20}$$

where $\mathbf{I}$ is an identity matrix. Because the coefficients matrix of Eq. (20) is singular, a normalizing condition is required in order to determine a unique eigenvector. There is an exact expression [14] that Daubechies wavelets satisfy, which is as follows:

$$\sum_k k^m \phi(x - k) = x^m + \sum_{k=1}^{m} (-1)^k \binom{m}{k} x^{m-k} \int_\infty \phi(x) x^k \,\mathrm{d}x. \tag{21}$$

Differentiating the above equation, we have

$$\sum_k k^m \phi^{(m)}(x - k) = m!; \tag{22}$$

Multiplying both sides of this equation by the characteristic function, we obtain

$$\sum_k k^m \int_\infty \chi_{[0,1]}(\xi)\phi^{(m)}(\xi - k)\,\mathrm{d}\xi = \int_\infty \chi_{[0,1]}(\xi) m!\,\mathrm{d}\xi \Rightarrow \sum_k k^m M_k^m = m!. \tag{23}$$

Supplying this normalizing condition to Eq. (20), one can get the connection coefficients M_k^0.

For $s > 0$, we find the formula according to Eq. (18) as follows:

$$(2^{m+1}\mathbf{I} - \mathbf{P})\mathbf{M}_k^m = \sum_r P_{r-2k+1} \sum_{s=1}^{m} \binom{m}{s} \mathbf{M}_r^{m-s}. \tag{24}$$

Solving this linearly independent inhomogeneous equation, we can obtain all the connection coefficients of Eq. (14). It should be pointed out that the technique used to calculate these load vectors is preferable as it requires less CPU time.

Once we have a technique for calculating the load vector, we also have a similar technique for calculating many other important integrals, such as the connection coefficients (15), which are necessary for the application of wavelet bases to two-dimensional WFE. These integrals can be obtained through solving the following equations:

$$\tau_{k,l}^{m,n} = 2^{m+n-1}\sum_{r,s}(p_{r-2k}\,p_{l-2s} + p_{r-2k+1}\,p_{l-2s+1})\tau_{r,s}^{m,n},$$

$$\sum_{k,l} k^m l^n \tau_{r,s}^{m,n} = m!n!. \tag{25}$$

These algorithms enhance the precision and speed of the computation of WFE.

4. The WFE equations for a thin plate

4.1. The bending equations for a thin plate

The generalized function of potential energy for a thin plate is [15]

$$\pi_p = \frac{1}{2}\int_\Omega\int \mathbf{K}^{\mathrm{T}}\mathbf{D}\mathbf{K}\,\mathrm{d}x\,\mathrm{d}y - \int_\Omega\int \mathbf{W}^{\mathrm{T}}\mathbf{q}\,\mathrm{d}x\,\mathrm{d}y, \tag{26}$$

where $\mathbf{K}$ is the generalized strain:

$$\mathbf{K} = \left[-\frac{\partial^2 w}{\partial x^2} - \frac{\partial^2 w}{\partial y^2} - 2\frac{\partial^2 w}{\partial x\,\partial y}\right]^{\mathrm{T}}, \tag{27}$$

$\mathbf{D}$ is the elastic matrix, $\mathbf{W}$ is the displacement of the thin plate and $\mathbf{q}$ is the load vector.

Defining the displacement of wavelet space,

$$w = \Phi(\mathbf{x})\otimes\Phi(\mathbf{y})\mathbf{d}. \tag{28}$$

Substituting Eq. (28) into Eq. (27), we obtain

$$\mathbf{K} = \begin{Bmatrix} -\phi''(x)\otimes\phi(y)\mathbf{d} \\ -\phi(x)\otimes\phi''(y)\mathbf{d} \\ -2\phi'(x)\otimes\phi'(y)\mathbf{d} \end{Bmatrix}. \tag{29}$$

Substituting Eqs. (28) and (29) into Eq. (26), we have

$$\pi_p = \tfrac{1}{2}\,\mathbf{d}^{\mathrm{T}}\mathbf{k}\mathbf{d} - \mathbf{d}^{\mathrm{T}}\mathbf{P}, \tag{30}$$

where

$$\begin{aligned}\mathbf{K} = {} & D(\boldsymbol{\tau}_y^{00}\otimes\boldsymbol{\tau}_x^{22} + \mu((\tau_y^{02})^{\mathrm{T}}\otimes\boldsymbol{\tau}_x^{02} + \boldsymbol{\tau}_y^{02}\otimes(\boldsymbol{\tau}_x^{02})^{\mathrm{T}}) \\ & + \boldsymbol{\tau}_y^{22}\otimes\boldsymbol{\tau}_x^{00} + 2(1-\mu)\boldsymbol{\tau}_y^{11}\otimes\boldsymbol{\tau}_x^{11}),\end{aligned} \tag{31}$$

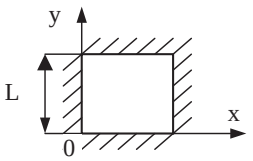

Fig. 1. The clamped thin plate.

$$\mathbf{P} = \int\int \mathbf{q}\phi^{\mathrm{T}}(\xi) \otimes \phi^{\mathrm{T}}(\zeta)\,\mathrm{d}\xi\,\mathrm{d}\zeta. \tag{32}$$

According to the theorem of potential energy, we obtain

$$\frac{\partial \pi_p}{\partial \mathbf{d}} = \mathbf{0} \Rightarrow \mathbf{K}\mathbf{d} = \mathbf{P}. \tag{33}$$

In the above equation, the stiffness matrix **K** and load vector **P** are made up of connection coefficients. Through solving Eq. (33), one can get the coefficients of wavelet space, and then substituting **d** into Eq. (28), the displacement of any point can be obtained.

4.2. Numerical results

The square thin plate clamped all sides is loaded with equal q, as shown in Fig. 1.

The bending rigidity is D. The deflection of the middle point is calculated based on WFE. Adopting Eq. (32) directly, and considering the boundary condition

$$w = w' = 0, \tag{34}$$

one can obtain the numerical result, 0.00126422 qL^4/D, which matches the exact solution 0.00126532 qL^4/D very well and the relative error of deflection is only 0.087%. This simple numerical result shows the accuracy of WFE method.

5. Numerical examples

While different order wavelets are used as interpolation functions, we can get different order wavelet elements, such as D3, D6, D8 and others [9]. In each class of element, for instance D6, there are different resolution wavelet elements D6j corresponding to the changing of the resolution of space V_j. The accuracy of the wavelet elements increases with the order of wavelet and the resolution j of space. The overall performance of the proposed wavelet elements is evaluated using a set of problems selected from the literature.

5.1. Cook's problem

The first evaluation is done with Cook's plane stress problem defined in Fig. 2.

It is the swept and tapered panel under shear load. There is no known analytical solution but the results for the 32×32 mesh may be used for comparison purposes [16]. The results obtained

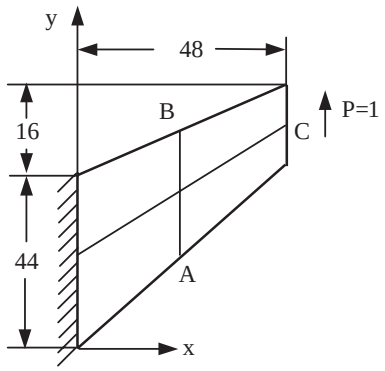

Fig. 2. Cook's problem ($E = 1$, $v = 1/3$).

Table 1
Stress results for Cook's problem

Element	σ_a—Maximum stress at A and σ_b—minimum stress at B					
Mesh	2×2		4×4		16×16	
	σ_a	σ_b	σ_a	σ_b	σ_a	σ_b
HG	0.0933	−0.1394	0.1628	−0.1566	0.2225	−0.1952
Q4	0.1281	−0.0916	0.1905	−0.1510	0.2358	−0.2002
D30	0.1801	−0.1765	0.2203	−0.1821	0.2359	−0.2005
D60	0.1872	−0.1836	0.2301	−0.1935	0.2359	−0.2010
Reference	$\sigma_a = 0.2359$			$\sigma_b = -0.2012$		

Table 2
Displacement results for Cook's problem

Element	v_c—Vertical deflection at C		
Mesh	2×2	4×4	16×16
HG	22.32	23.23	23.91
Q4	11.85	18.3	23.43
D30	22.25	23.19	23.65
D60	23.13	23.67	23.91
Reference	23.91		

with several elements under different meshes are given in Tables 1 and 2. Results for HG and Q4 elements are taken from [17]. D30 is a three-order wavelet element in space V_0 while D60 is a six-order wavelet element.

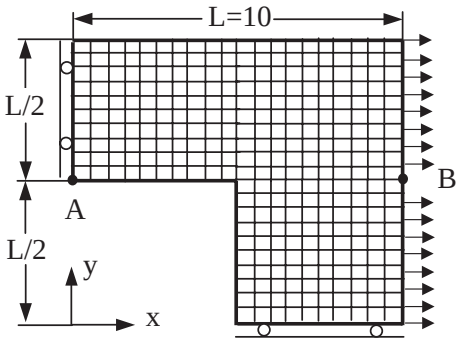

Fig. 3. *L*-shape domain problem (20×20 mesh).

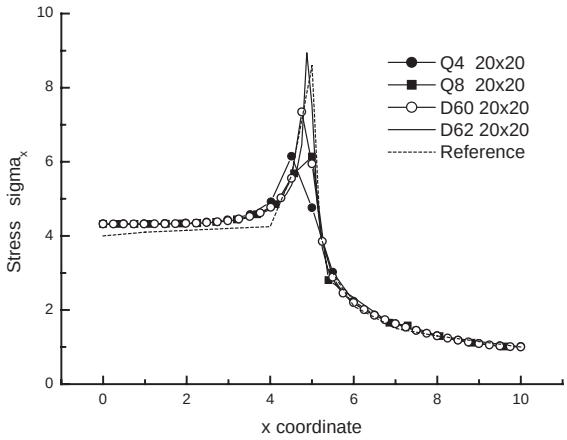

Fig. 4. Stress σ_x along *A–B*.

It is generally observed that the results show very good numerical accuracy for both displacements and stresses, even for relatively coarser finite-element meshes. The wavelet element D60 has excellent performance.

The convergence in the energy norm is the natural convergence test for the FEM. It is common practice in the literature, however, to examine convergence of the finite-element solution by analyzing the displacements at characteristic points [18]. Table 1 shows that with the increasing of the order of wavelet and the number of mesh, wavelet elements have good convergence properties.

5.2. *L*-shape domain problem

The problem defined in Fig. 3, an *L*-shape domain in plane stress condition, is proposed by Zienkiewicz [15,19] as a test case for the ability of elements to calculate the corner stress. Young's modulus $E = 1500/16$, Poisson rate $u = 0.25$. Different elemental results for the fixed mesh 20×20 are shown in Fig. 4, and the zoom-in stress results in Fig. 5. Q4 is the traditional *Lagrange* linear interpolation functions for the four-node rectangular element, and Q8 is higher-order version of Q4.

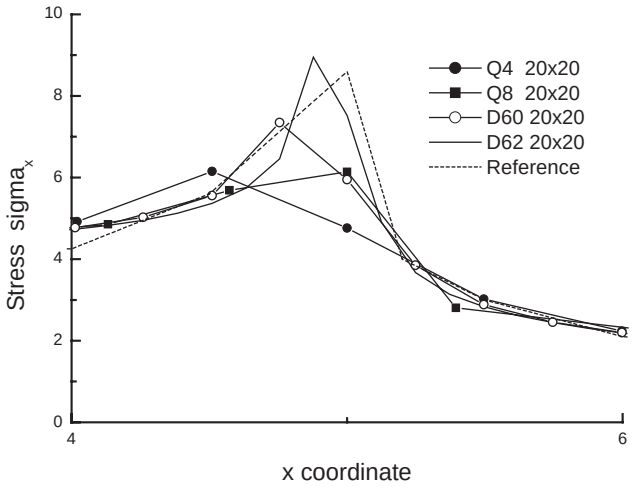

Fig. 5. The zoom-in zones.

D60 and D62 are six-order wavelet elements in space V_0 and V_2, respectively. The reference stress σ_x along A–B is taken from [15]. The D62 element yields the best result for this problem. Considering Eq. (4) again, we can see, the nested property indicates that as j gets larger, more information or more accuracy is revealed by an approximation; this multi-resolution refining strategy is easily applied through the fast reconstruction algorithms of wavelets [12]. As we know, for smooth solution problems, p-refinement is converged rapidly. But the presence of singularities may decrease the rate of convergence significantly; while the multilevel and approximation properties of the scaling function of the multi-resolution analysis provide computational efficiency and accuracy of numerical solution. From Fig. 5 we can see that this strategy is superior to p-refinement.

5.3. Mesh distortion

To assess the sensitivity of the new elements to mesh distortion, a coarse mesh modeling a clamped square plate is used. The bending rigid is equal to 1. Two types of distortions are introduced [18]. The center node of the mesh is moved along the main diagonal of the plate as shown in Fig. 6(a), and the center node is moved parallel to the edge in Fig. 6(b). The results are shown in Figs. 5 and 6, respectively. The elements CRB1, CRB2 and S1 are taken from [18]. From the results we can see that the D62 element appears less sensitive to element layout (Figs. 7 and 8).

6. Paper steady-state thermal analysis

Office machines such as printers and copiers have been widely used in our daily life. However, paper jam is an annoying problem that these machines often encounter. Previous researches related to the static and dynamic mechanical properties of office paper have been analyzed [20,21]. Another important problem is the quality of fixing process, in which office paper with carbon powder is fed through two rollers with high temperatures, and then carbon powder is fixed on it. The key for

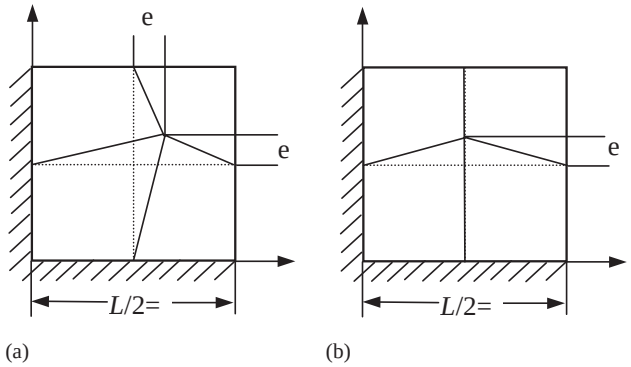

Fig. 6. Mesh distortion: (a) symmetric and (b) asymmetric.

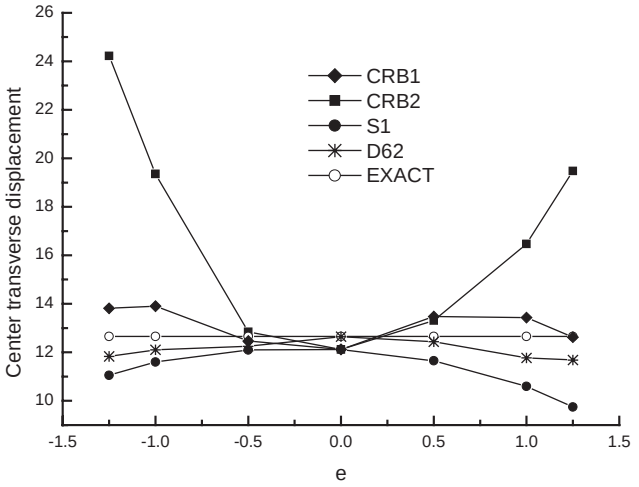

Fig. 7. Sensitivity to mesh distortion, symmetric.

studying the quality of fixing process is to analyze the internal temperature distribution of office paper, which also provides the researching bases for office paper thermal–structural analysis and reasonable design of paper feeding mechanism.

The steady-state thermal conduction equation of paper is expressed as follows:

$$k\frac{\partial^2 T}{\partial x^2} + k\frac{\partial^2 T}{\partial y^2} = 0, \tag{35}$$

where T denotes the temperature and k is the heat conductivity.

The boundary conditions are:

$$T(x,t) = T_{\mathrm{r}} \quad \text{(contacting with rollers)}, \tag{36}$$

$$k\frac{\partial T}{\partial x} = h(T_{\mathrm{a}} - T) \quad \text{(contacting with air)}, \tag{37}$$

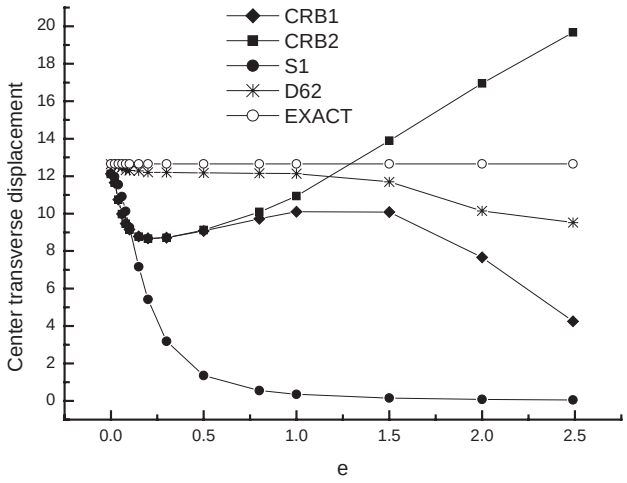

Fig. 8. Sensitivity to mesh distortion, asymmetric.

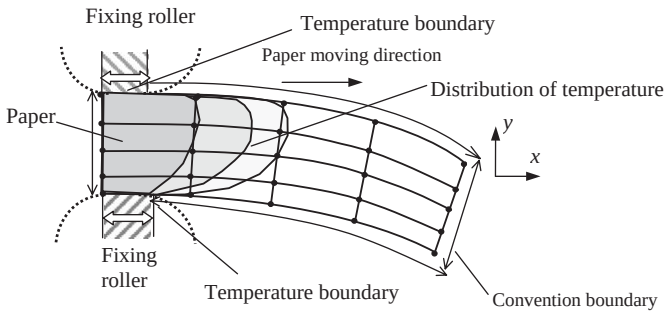

Fig. 9. The thermal analysis of office paper.

where T_r and T_a denote the temperature of fixing rollers and air, h denotes the convection coefficient between paper and air.

According to the working status, the boundary condition of the type6200 paper contacting with the rollers is temperature boundary, as shown in Fig. 9. The temperature of the rollers is 453 K and the corresponding paper length is 4 mm; the other is convection boundary, the surroundings temperature is 293 K, the convection coefficient is 13 W/m^{2}K, and the heat conductivity is 0.094 W/mK.

In order to establish special CAD/CAE system for paper feeding mechanism, we have developed FEM programs, of which the analysis ability is equal to current finite-element software, such as ANSYS, by using eight-node quadrilateral isoparametric elements to analyze the paper characteristics with FORTRAN POWERSTATION. Through analysis, we discover that there is 0.5% numeric distortion caused from temperature change besides the point of x coordinate equal to 4.

From the numerical results of wavelets of elements solving for L-shape domain problem in Section 5, we can see that the local approximation and multi-resolution merits of orthnormal, compactly supported wavelets make the WFE competitive especially for singularity problems. When the

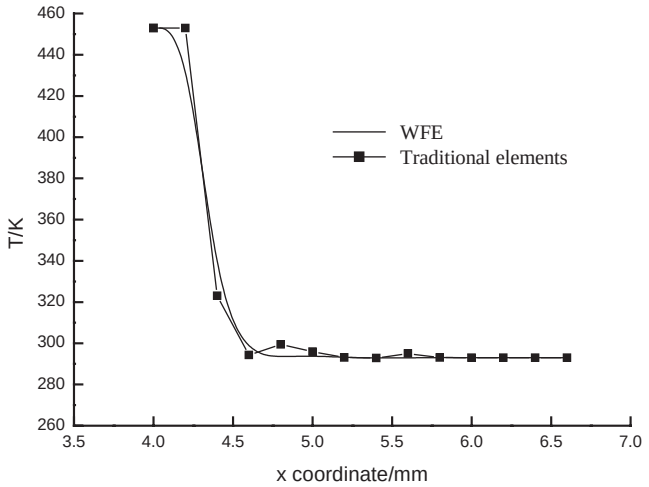

Fig. 10. The analysis results.

Daubechies scaling functions are used as trial functions to analyze the temperature distribution and the boundary conditions imposed by the methods [22], this phenomenon of numerical distortion can be avoided. As shown in Fig. 10, from the paper length of 4.5–6 mm, the analysis results of WFE is more reasonable, which can provide accuracy numerical simulation for the office paper.

7. Conclusions

This paper has constructed two-dimensional wavelet finite element, which is formulated in terms of Daubechies wavelet basis functions. An efficient integral method to calculate stiffness and load matrices is presented by employing two-scale equations and normalization conditions satisfied by Daubechies wavelets. Although the Daubechies scaling functions have no explicit expression, their interpolation can approximate any high-order polynomial accurately. Based on WFE the bending equations for a thin plate are derived, and the precision of WFE is verified through the corresponding numerical result.

Because of the orthonormal, compactly supported and nesting properties of the Daubechies wavelets, the resulting elements are shown to perform well on a set of standard problems. It also shows that wavelets bases are attractive for multi-resolution refinement. Through the analysis of the internal temperature distribution of office paper, we discover that WFE has good ability to deal with singularity problems.

Acknowledgements

This work is supported by National Natural Science Foundation of China (No. 50175087) and Doctorate Foundation of Xi'an Jiaotong University (No. DFXJU1999-6).

References

[1] Liang Guoping, He Jiangheng, Generalized finite element method, Adv. Mech. 25 (1995) 562–565 (in Chinese).
[2] W. Dahmen, Wavelet methods for PDEs—some recent developments, J. Comput. Appl. Math. 128 (2001) 133–185.
[3] L. Castro, J. Freitas, Wavelets in hybrid-mixed stress elements, Comput. Methods Appl. Mech. Eng. 190 (2001) 3977–3998.
[4] S. Jaffard, P. Laurencot, Orthonormal wavelets, analysis of operators and applications to numerical analysis, in: C. Chui (Ed.), Wavelets: A Tutorial in Theory and Applications, Academic Press, New York, 1992, pp. 543–601.
[5] J. Ko, A.J. Kurdila, A class of finite element methods based on orthonormal compactly supported wavelets, Comput. Mech. 16 (1995) 235–244.
[6] W. Danmen, C.A. Micchelli, Using the refinement equation for evaluating integrals of wavelets, SIAM J. Numer. Anal. 30 (1993) 507–537.
[7] M.Q. Chen, C. Hwang, Y.P. Shih, The computation of wavelet-Galerkin approximation on a bounded interval, Int. J. Numer. Methods Eng. 39 (1996) 2921–2944.
[8] P. Monasse, V. Perrier, Orthonormal wavelet bases adapted for partial differential equations with boundary conditions, SIAM J. Math. Anal. 29 (1998) 1040–1065.
[9] J. Ma, J. Xue, S. Yang, Z. He, A study of the construction and application of a Daubechies wavelet-based beam element, Finite Elements Anal. Design, in press [doi:10.1016/S0168-874X(02)00141-5].
[10] Yang Shengjun, Theory of finite element of B-spline wavelet on the interval and its engineering application, Ph.D. Thesis, School of Mechanical Engineering, Xi'an Jiaotong University, 2002 (in Chinese).
[11] S. Mallat, Wen Liang Hwang, Singularity detection and processing with wavelets, IEEE Trans. Inf. Theory 38 (1992) 617–643.
[12] I. Daubechies, Orthonormal basis of compactly supported wavelets, Commun. Pure Appl. Math. 41 (1988) 909–996.
[13] I. Daubechies, Recent results in wavelet applications, J. Electron. Imaging 7 (1998) 719–724.
[14] G. Beylkin, On the representation of operators in bases of compactly supported wavelets, SIMA J. Numer. Anal. 6 (1992) 1716–1740.
[15] O.C. Zienkiewicz, R.L. Taylor, The Finite Element Method, 4th Edition, McGraw-Hill Book Company, London, 1988.
[16] P.G. Bergan, C.A. Felippa, A triangular membrane element with rotational degrees of freedom, Comput. Methods Appl. Mech. Eng. 50 (1985) 25–69.
[17] R.D. Cook, Improved two-dimensional finite element, J. Struct. Division 100 (1974) 1851–1863.
[18] S.L. Weissman, R.L. Taylor, Resultant fields for mixed plate bending elements, Comput. Meth. Appl. Mech. Eng. 79 (1990) 321–355.
[19] O.C. Zienkiewicz, J.Z. Zhu, Accuracy and adaptivity in FE analysis: the changing face of practical computations, in: Y.K. Cheung (Ed.), Computational Mechanics, Rotterdam, Balkema, 1991, pp. 3–12.
[20] Yang Shengjun, Ma Junxing, He Zhengjia, Damping property of free vibration for office equipment paper, J Xi'an Jiaotong University 34 (2000) 48–51 (in Chinese).
[21] Ma Junxing, Yang Shengjun, He Zhengjia, et al., Mechanical properties of office paper analyzed by using nonlinear finite element method, J. Xi'an Jiaotong University 34 (2000) 67–71 (in Chinese).
[22] S.L. Ho, S.Y. Yang, Wavelet-Galerkin method for solving parabolic equations in finite domains, Finite Elements Anal. Design 37 (2001) 1023–1037.